



HAL
open science

Sclerochronological and geochemical study of the carpet shell *Ruditapes decussatus* in archaeological contexts: A potential tool for season of collection and coastal paleo-temperature

Marc Gosselin, Catherine Dupont, Céline Poulain, Xavier Le Coz, Grégor Marchand, Christine Paillard, Yves-Marie Paulet, François Pustoc'H, Yves Gruet

► **To cite this version:**

Marc Gosselin, Catherine Dupont, Céline Poulain, Xavier Le Coz, Grégor Marchand, et al.. Sclerochronological and geochemical study of the carpet shell *Ruditapes decussatus* in archaeological contexts: A potential tool for season of collection and coastal paleo-temperature. *Journal of Archaeological Science: Reports*, 2023, 48, pp.103827. 10.1016/j.jasrep.2023.103827 . insu-03955850

HAL Id: insu-03955850

<https://insu.hal.science/insu-03955850>

Submitted on 30 Jan 2023

HAL is a multi-disciplinary open access archive for the deposit and dissemination of scientific research documents, whether they are published or not. The documents may come from teaching and research institutions in France or abroad, or from public or private research centers.

L'archive ouverte pluridisciplinaire **HAL**, est destinée au dépôt et à la diffusion de documents scientifiques de niveau recherche, publiés ou non, émanant des établissements d'enseignement et de recherche français ou étrangers, des laboratoires publics ou privés.

1 Sclerochronological and geochemical study of the carpet shell *Ruditapes decussatus* in archaeological
2 contexts: a potential tool for season of collection and coastal paleo-temperature

3

4 ¹ Marc Gosselin, ¹ Catherine Dupont, ² Céline Poulain, ³ Xavier Le Coz, ¹ Grégor Marchand, ² Christine
5 Paillard, ² Yves-Marie Paulet, ¹ François Pustoc'h, ⁴ Yves Gruet

6 ¹ CNRS, Université de Rennes, UMR 6566 CReAAH « Centre de Recherche en Archéologie
7 Archéosciences Histoire » 35000 Rennes, France

8 ² LEMAR, UMR 6539 CNRS/UBO/IRD/IFREMER, Institut Universitaire Européen de la Mer, Place Nicolas
9 Copernic, 29280 Plouzané, France

10 ³ Géosciences Rennes Atelier Géomatériaux, UMR 6118 CNRS, OSUR, Université de Rennes, 35042
11 Rennes cedex, France

12 ⁴ Honorary researcher of the Université de Nantes, France

13

14 Keywords

15 *Ruditapes decussatus*, Bivalve Mollusk, Shell Midden, Sclerochronology, Sclerochemistry, Seasonality,
16 Paleo-temperature, Mesolithic, European Atlantic coast

17 Abstract

18 Specimens of the carpet shell *Ruditapes decussatus* from the Mesolithic shell midden (6th millennium
19 BC) of Beg-an-Dorchenn (Brittany, France) were studied in order to assess their period of collection as
20 well as provide some insight on Paleo-temperature reconstructions. Cross sectioned shells display very
21 clear growth structures allowing an assessment of a growth rhythm of 2 increments per lunar day.
22 From this temporal framework, daily growth increments and winter annual growth breaks were
23 characterized. Our results show the *R. decussatus* shells were typically collected in the early spring
24 period. Chemical analyses of shell carbonates were also performed to assess a preliminary range of
25 potential sea temperature data from oxygen isotopes values ($\delta^{18}\text{O}_{\text{shell}}$). $\delta^{18}\text{O}_{\text{shell}}$ shows seasonal
26 variations but do not record the whole seasonal temperature range as *R. decussatus* have a growth
27 break during winter. However, results show predicted SSTs within the range of expected values. Thus,
28 *R. decussatus* is particularly suited for paleo-environmental reconstructions at high temporal
29 resolution such as seasonal timescales. Additional sclerochronological and chemical research on
30 additional carpet shells and also other mollusk species from Beg-an-Dorchenn or other Mesolithic shell

31 middens along the European Atlantic coast should be considered. Such studies will contribute to the
32 understanding of the seasonal occupation patterns of the last hunter-gatherers of the European
33 Atlantic coast as well as the climate variability at the Mesolithic-Neolithic transition.

34 I. Introduction

35 The study of hunter-gatherer populations involves a deep understanding of their interactions with the
36 local environment, especially concerning their spatial and temporal residential behaviors. The
37 particular activity pattern of these communities (*i.e.* dependence on wild resources) implies a close
38 interdependency with climatic variability and involves numerous environmental parameters at
39 different timescales and periodicities (*e.g.* daily and monthly tidal cycles, seasonal faunal migrations,
40 annual primary production) (Yesner 1980, Testart 1982, Zvelebil 1986, Moss 1993).

41 Archaeological and ethnographical studies show that coastal hunter-gatherer populations had an
42 extensive knowledge of their terrestrial as well as maritime environments (Thomson 1939, Yesner
43 1980, Dupont and Marchand 2016). For the latter, the sea can bring a large diversity of wild resources
44 such as mammals, fishes, crustaceans, mollusks, seaweed, and lithic materials. The remains of their
45 activities (*i.e.* their waste products) create deposits rich in critical information that permits
46 archaeologists to improve the understanding of these maritime populations (Milner et al. 2007,
47 Claassen 1998). Shell deposits and shell middens are important faunal depositional environments
48 within archaeological sites, especially during the Mesolithic along the European Atlantic coast
49 (Gutiérrez-Zugasti et al. 2011).

50 Thus, *via* qualitative and quantitative diversity analyses, archaeomalacological studies give information
51 about paleoenvironments, human diets or human behavior (Claassen 1998, Bar-Yosef Mayer 2005,
52 Dupont 2006, Szabo et al. 2014). In this framework, sclerochronology, the study of accretional hard
53 elements of biological organisms, provides useful insights on the species life traits (*e.g.* rhythm and
54 variation of growth) as well as on the environment in which individuals grew (Buddemeier 1978, Jones
55 1983, Bessat and Tabeaud 1998, Schöne 2008, Schaffer et al. 2011, Wanamaker et al. 2011, Gosselin
56 et al. 2013). Based on mollusk species, sclerochronological studies in archaeological shell middens offer
57 the possibility to assess their season of collection and thus to deduce periods of coastal settlement
58 residence, or fishing activity, by human communities. Moreover, complementary chemical analysis
59 along the mollusk shells growth axis (sclerochemistry) gives additional clues on paleoclimatic and
60 paleoenvironmental parameters such as sea surface temperature (SST), primary production or salinity
61 (Andrus 2011). Along the European Atlantic coast more than 240 Mesolithic shell middens have been
62 reported but evidence of clear residence pattern is still scarce (Dupont 2016). Among those
63 settlements, the bivalve *Ruditapes decussatus* usually appears in the top three most abundant mollusk

64 species (Gutiérrez-Zugasti et al. 2011). This Veneridae is a widespread diachronic species with a large
65 latitudinal modern distribution from Norway to Portugal (Quéro and Vayne 1998). Moreover, its shell
66 thickness and size provide a substantial area for potential experiments making it particularly suitable
67 to combine sclerochronological and geochemical analysis. Indeed, to date, studies focused on mollusks
68 have typically employed only one method of investigation (sclerochronology or geochemical analysis)
69 (Mannino et al. 2003, Deith 1983, Brock and Bouget 1989, Milner 2005). Here, we jointly apply
70 sclerochronology and geochemistry to the archaeological *R. decussatus* shells from the Mesolithic
71 settlement of Beg-an-Dorchenn (Brittany, France). Such studies have already been conducted on
72 modern shells of the sympatric and currently commercialised *R. philippinarum* species (Poulain 2010,
73 Poulain et al. 2010, Poulain et al. 2011). Sclerochronological studies showed that *R. philippinarum* daily
74 growth follows a tidal rhythm (Poulain et al. 2011). Sclerochemical studies of *R. philippinarum* shells
75 lead to an equation between the $\delta^{18}\text{O}$ values of sea water ($\delta^{18}\text{O}_w$) and salinity (Poulain 2010). However,
76 no SST proxy derived from oxygen isotopes samples currently exists. To our knowledge there is no
77 previous work on modern or archaeological specimen of the native grooved carpet shell clam *Ruditapes*
78 *decussatus* involving shell oxygen isotopes. Thus, there is no modern calibration study for
79 palaeotemperature and one must keep in mind throughout the present study that physiological
80 processes may be involved in the fractionation processes.

81 This paper aims to transfer knowledge gained from studying modern shells of *R. philippinarum* to
82 archaeological shells of *R. decussatus*, enabling us to use the latter as a recorder of Mesolithic period
83 human activities along the European Atlantic coasts. First, we conduct structural observations of the
84 archaeological shells to 1) deal with potential diagenesis issues, 2) characterize increment readability
85 and 3) confirm the temporal framework of shell growth patterns. From this basis, two shells (BAD-5
86 and BAD-18) were chosen to test jointly sclerochronological and biogeochemical analysis in order to
87 identify the seasonality of shellfish collections and discuss the paleoenvironmental reconstruction
88 process.

89 II. Materials and Methods

90 II.1. Material

91 II.1.1. Species biology

92 The native European carpet shell *Ruditapes decussatus* (Linnaeus, 1758) is a mollusk from the
93 Veneridae family living in the intertidal zone; from the mean high water level to the upper sublittoral
94 level. This bivalve is a filter feeder and deposits feeder species which burrows in mud, sand or even
95 muddy gravel at a maximum depth of 15 cm. Its growth, up to 8 cm (mean 4-5 cm), is mainly controlled

96 by environmental parameters such as sea temperature and food availability. *R. decussatus* is an
97 euryhaline (20-50 ppt, optimum 30 ppt) (Le Treut 1986) and eurythermal (10° C-32° C, optimum 20-
98 25° C) species (Sobral and Widdows 1997).

99 II.1.2. Archaeological site

100 The carpet shells studied in this paper came from one of the few French shell middens of the
101 Mesolithic: Beg-an-Dorchenn (Brittany, France, Figure 1. A-B). This shell-midden is a key archaeological
102 site to understand the Neolithization process along the French Atlantic coast (Figure 3.). Along the
103 coast, only 6 sites are known for the Late Mesolithic. Beg-an-Dorchenn shows a clear dependence of
104 the hunter-gatherers on the marine environments accessible in the vicinity of the settlement which
105 was a maximum of one kilometre from the foreshore during occupation (Dupont et al. 2009). The wide
106 diversity of remains of wild exploited resources demonstrates an expert use of the local biodiversity.
107 Moreover, the temporal addition of the different seasonally available animal and vegetal exploited
108 resources shows that this human population was able to survive throughout the year at the site
109 (Dupont et al. 2009). So, the question of the permanent residence (nomadic VS sedentary) of this
110 Mesolithic population can be asked.

111 Beg-an-Dorchenn shell-midden thickness decreased from more than one meter during the 19th century
112 (Du Chatellier 1881) to 30 cm at the end of the 20th due to erosion (Figure 1. C). A supplementary
113 sample excavation was performed in 2001 with an interdisciplinary focus in mind (Dupont et al. 2010)
114 (see details in supplementary material 1). The aspect of the shell-midden is a black organic layer (Figure
115 2. A-B). It was composed of marine resources (shells, crabs, fishes, birds and mammals), terrestrial
116 remains (birds, mammals, charcoals) and flints. A total of 26 kg of shells have been obtained from the
117 sieved sample of 2001. The total minimum number of individuals (MNI) has been evaluated to 13,324
118 individuals of shells. 6.6% of them are *R. decussatus*. Radiocarbon dating attributes this Late Mesolithic
119 occupation from the middle to the end of the sixth millennium BC (Marchand et al. 2009). Among the
120 50 fragments of the most complete carpet shells coming from Beg-an-Dorchenn, two very well-
121 preserved valves of *Ruditapes decussatus* have been chosen for sclerochronological and biogeochemical
122 analysis: a left one (BAD-5 from level 7) and a right one (BAD-18 from level 5)

123 II.2. Methods

124 II.2.1. Preparation of shell cross section

125 Incremental growth structures can be observed under a microscope from a shell cross section. One
126 valve of each specimen of *R. decussatus* was cut along the axis of maximum growth from the umbo to
127 the ventral margin. The valve was preliminarily embedded in epoxy resin (Araldite 2020©). Three cuts

128 are made perpendicular to the growth lines with a high concentration diamond-coated 0.43 mm metal
129 blade (430CA Ø 152 mm) mounted on a low speed precision saw (Accutom 50, Struers®, 2700 rpm,
130 feed speed 0.075 mm/s). Two consecutive embedded thin sections of 1.1 mm thickness are obtained
131 and glued with Araldite on a sand blast glass slide. Next, the thickness and planeness of the thin section
132 is adjusted to obtain a planar and smooth surface. This step enables growth structure observation of
133 the shell by polishing the thin section with decreasing size grits of Al₂O₃ powders (1200, 2400, 4000
134 grain sizes) then with diamonded paste (Ø 3 and 1 µm) (Grinder-Polisher Tegra Force 5 Struers ©).
135 Between each grinding/polishing step, thin sections were cleaned by ultrasonic bathing in MilliQ water
136 (Bioblock Scientific ©). Thus, embedding, cutting and polishing steps leads to a thin section of the shell
137 containing all its lifespan from birth to death.

138 Shell structure was observed by scanning electron microscope with chemical analysis by Raman
139 spectrometry (see details in supplementary material 1).

140 II.2.2. Growth microstructure analysis

141 Growth microstructures were observed from the outer shell layer of the thin section under an optical
142 microscope (Leica S8AP0) at 40-100x magnification with reflective light coupled with a camera (Leica
143 EC3) to take digital photographs. Growth increment thicknesses were then measured from the ventral
144 margin to the umbo direction using the image analysis software Visilog (V6.481) with an adapted
145 sclerochronological macro (Noesis Co.) (Gosselin et al. 2007). One growth increment is defined as the
146 couple of one thin dark growth line and one larger white growth line.

147 II.2.3. Shell geochemistry

148 Oxygen isotope analyses in mollusk shells ($\delta^{18}\text{O}_{\text{Shell}}$) reflect sea surface temperature (SST) and $\delta^{18}\text{O}$
149 seawater ($\delta^{18}\text{O}_{\text{W}}$) variations (Urey et al. 1951). $\delta^{18}\text{O}$ is a measure of the ratio of ¹⁸O to ¹⁶O relative to a
150 standard material (VPDB). Carbonate oxygen stable isotopic ratios depend on two main factors: i)
151 Water temperature during the calcification process ii) the oxygen isotope composition of the
152 surrounding water. $\delta^{18}\text{O}_{\text{W}}$ variability encompass all the water cycle processes (*i.e.* evaporation,
153 condensation, precipitation, surface run off) and can also often reflect salinity variations of the sea
154 waters (Epstein and Mayeda 1953).

155 In this study, $\delta^{18}\text{O}_{\text{Shell}}$ analysis were performed in the outer shell layer of the thin section by drilling
156 (Micromill NewWave ©) with a drill bit tip diameter of 200 µm. 83 powder samples from 33 to 94 µg
157 were collected from the corresponding shell portion where sclerochronological analyses were
158 performed. The drilled spots had a mean diameter of 380 ± 68 µm and a maximum depth of 400 µm
159 while the distance between two consecutive holes was 68 ± 45 µm. Powder samples were then

160 processed in a Thermo Finnigan MAT 253 Isotope ratio mass spectrometer coupled to a Gas bench II.
161 The calibration standard is NBS-19 ($\delta^{18}\text{O} = -1.91 \text{ ‰}$) with an internal precision of 0.05 ‰ and an
162 accuracy (1σ) of 0.07 ‰. $\delta^{18}\text{O}$ are expressed relative to the Vienna Pee Dee Belemnite international
163 standard (VPDB) and given as per mil (‰). In the absence of a specific paleotemperature
164 reconstruction equation for those two aragonitic species, we chose the corrected equation of Böhm
165 et al. (2000) which is built from $\delta^{18}\text{O}$ datasets of different bioaragonitic seawater invertebrates.
166 Moreover, in order to account for the seasonal variability of salinity on the $\delta^{18}\text{O}$ values of sea water
167 we worked with the $\delta^{18}\text{O}_w / \text{salinity}$ equation of Poulain (2010).

168 II.2.4. Catch seasonality methodology

169 In order to assess the seasonality of shellfish collections and thus the presence of human population
170 at the coastal site, we used two different methods. First, from the sclerochronological study we
171 counted the number of increments after the last annual growth break. Second, from the
172 sclerochemical study, we used the quartile method (Mannino et al. 2003, Prendergast et al. 2016). For
173 the latter, the annual $\delta^{18}\text{O}$ variations were calculated from the third year of growth of BAD-5 shell and
174 from the fourth year of growth of BAD-18 shell when the specimens displayed a maximum of growth
175 days among a year (10 and 9 months respectively).

176 III. Results

177 III.1. Shell diagenesis and growth line readability

178 Structural and chemical analyses were performed on archeological shells. Raman analyses were carried
179 out on a thin section on different spots of the shell of BAD-5. Raman spectra reveal that the calcium
180 carbonate composition of the archaeological shells is aragonite (Wavelength 568 nm, wave number
181 peaks at 155, 205, 271, 704 cm^{-1} and 1085 cm^{-1}). Those results are very similar to those found in
182 modern shells of *Ruditapes decussatus* and *R. philippinarum* (Trinkler et al. 2011).

183 Fragments of *R. decussatus* broken by hand were observed on SEM. Three archaeological shells from
184 Beg-an-Dorchenn have been observed including shell BAD-18. They display two layers of aragonite: a
185 homogeneous inner layer and a prismatic outer layer (Figure 4) Growth increments exhibit an
186 exceptional readability for these 6th millennium BC specimens.

187 III.2. Growth analysis: Time frameworks, periodicities, aging

188 Growth marks of the two shells of *Ruditapes decussatus* were counted and inter-mark distances
189 measured in order to build their respective growth trajectory curves from the high frequency analysis
190 of the growth increments of the thin sections to the external notches of the valves (Figure 5 and Table

191 1). The two shells of *Ruditapes decussatus* were nearly of the same size (*i.e.* 30.6 mm and 27.7 mm
192 along the maximum growth axis for BAD-5 and BAD-18 respectively).

193 III.2.1. From annual to tidal growth marks

194 Depending on the degree of growth line readability, the sclerochronological work took place along
195 almost all the thin section of the BAD-5 valve (3.3 cm for 1388 cumulated growth increments) while
196 the BAD-18 valve was studied over the last 1 cm of cumulated growth (657 increments) (Figure 5 B.).
197 The annual growth marks of each shell were investigated by observing their external surface as well as
198 the cross sections (Figure 5 A-B). They underline a break, or a drastic slowing, of growth; probably
199 attributable to the low sea temperature and/or low food availability occurring during winter. Those
200 annual growth marks are characterized by a V shape notch at the outer shell layer in cross section and
201 as a groove at the external shell surface. They usually appear during a period of low mean increment
202 thickness with a slow growth decrease before the notch and a fast increase after the notch (Sato,
203 1999). Each shell displays a total of 4 breaks following the annual growth marks criteria (N1 to N4 in
204 Table 2. and Figure 5.). Thus BAD-5 and BAD-18 are around 4 years old with different growth duration
205 depending on the year.

206 Indeed, while BAD-5 and BAD-18 exhibit a common increment thickness range between 5 and 80 μm ,
207 their distributions ($24.0 \pm 13.4 \mu\text{m}$ and $15.1 \pm 7.0 \mu\text{m}$ respectively) are significantly different (Wilcoxon-
208 Mann-Whitney test $U = 2.673 \times 10^5$; $P < 0.0001$) (Figure 5 C.). In the same line, BAD-5 shows larger
209 increments than BAD-18 in their last 1 cm of growth ($19.3 \pm 8.9 \mu\text{m}$ and $15.1 \pm 7.0 \mu\text{m}$ respectively;
210 Wilcoxon-Mann-Whitney test $U = 1.184 \times 10^5$; $P < 0.0001$). The ontogeny of the bivalve has an effect on
211 its growth: as the shells grow older, their mean growth increment thickness as well as their length of
212 the growth season decrease (Gosling 2003).

213 Between the third and fourth annual mark of BAD-18 a total of 510 increments were counted
214 suggesting a growth rhythm of two daily increments that may be influenced by tidal periodicity.
215 Indeed, modern tidal cycle in Brittany is semi-diurnal with two daily low/high tides. Thus, tidal growth
216 increments analysis of BAD-5 suggests a growth duration of 7, 10 and 5 months during 2nd, 3rd and 4th
217 year respectively while BAD-18 shows 9 months of incremental growth in its 4th year. Other tidal cycles
218 such as the neap/spring tide succession with a fortnightly periodicity are not observed from the high-
219 resolution growth patterns of the two *R. decussatus* archaeological shells (REDFIT spectral analysis on
220 tidal daily increments with software PAST V3.22).

221 III.3. Oxygen isotopic analysis

222 $\delta^{18}\text{O}_{\text{Shell}}$ mean sample values are statistically similar in BAD-5 and BAD-18 (Wilcoxon-Mann-Whitney
223 test $U = 538$; $P = 0.33$) even if BAD-5 $\delta^{18}\text{O}_{\text{Shell}}$ data show a larger range of values (Table 2 and Figure 5.
224 D). They follow sinusoidal shapes with a range between -0.78 and 1.02 ‰. In BAD-5, the 2nd and 3rd
225 years of incremental growth are negatively correlated with the related $\delta^{18}\text{O}_{\text{Shell}}$ values while those
226 parameters are positively correlated during the 4th year. In fact, a small but significant negative
227 correlation is observed between $\delta^{18}\text{O}_{\text{Shell}}$ values and growth increment thickness (Spearman
228 correlation test, $P < 0.001$, $R^2_{\text{BAD-5}} = 0.115$, $R^2_{\text{BAD-18}} = 0.144$). The positive correlation between the third
229 and the fourth growth break in BAD-5 may be the results of fresh water impact. Indeed, due to
230 physicochemical processes, the $\delta^{18}\text{O}_{\text{w}}$ is correlated to the salinity (Epstein and Mayeda 1953, Chauvaud
231 et al. 2005).

232 The annual growth marks of each shell are interpreted as negative environmental impacts occurring
233 during winter. During those breaks/slowing of growth, the corresponding $\delta^{18}\text{O}_{\text{Shell}}$ values are high,
234 implying low temperature periods which are in accordance with wintry conditions (Figure 5. C, D). An
235 estimate of paleo-SST was made using the corrected equation of Böhm et al. (2000) which was built
236 from $\delta^{18}\text{O}$ datasets of different bioaragonitic marine invertebrates [$\text{SST} = 20.0 - 4.42 \times (\delta^{18}\text{O}_{\text{Shell}} - (\delta^{18}\text{O}_{\text{w}} - 0.2 \text{ ‰}))$]
237 with the sea surface temperature expressed in ° C (SST), the $\delta^{18}\text{O}$ values in ‰ for the
238 aragonite shell ($\delta^{18}\text{O}_{\text{Shell}}$) and the sea water ($\delta^{18}\text{O}_{\text{w}}$). $\delta^{18}\text{O}_{\text{w}}$ is corrected by -0.2 ‰ to reflect unit change
239 from SMOW to PDB. For a $\delta^{18}\text{O}_{\text{w}}$ parameter set as a constant, a $\delta^{18}\text{O}_{\text{Shell}}$ variation of 1 ‰ shift is
240 equivalent to a 4.42° C variation in SST and the spectrometer accuracy of 0.07 ‰ is equivalent to 0.31°
241 C.

242 In order to account for the seasonal variability of salinity on the $\delta^{18}\text{O}$ values of sea water ($\delta^{18}\text{O}_{\text{w}}$), we
243 used the following equation described by Poulain (2010): $\delta^{18}\text{O}_{\text{w}} = 0.144 \times \text{Salinity} - 4.707$ ($N=35$,
244 $R^2=0.97$, $P_V < 0.001$) with the salinity values of Locmariaquer (distant of ± 100 km East from BAD site).
245 The maximum salinity of 35 ppt and minimal winter values of 27.5 ppt gave respectively a “seasonal”
246 $\delta^{18}\text{O}_{\text{w}}$ value of 0.333 ‰ and -0.747 ‰. During the desalinated winter period some isolated low values
247 of 19.5 may occur with a corresponding calculated value of -1.899 ‰. This latter salinity value is close
248 to the minimal salinity that *R. decussatus* can physiologically managed (Le Treut 1986).

249 With $\delta^{18}\text{O}_{\text{w}} = 0$ ‰ (standard mean ocean water), the reconstructed SST were $20.80 \pm 1.87^\circ \text{C}$ (min
250 16.37°C ; max 24.35°C) and $21.29^\circ \text{C} \pm 1.82^\circ \text{C}$ (min 18.47°C ; max 23.81°C) for BAD-5 and BAD-18
251 respectively. The reconstructed SST from BAD-5 $\delta^{18}\text{O}_{\text{Shell}}$ were also calculated with $\delta^{18}\text{O}_{\text{w}}$ “seasonal”
252 values for warm/high salinity (mean $20.50^\circ \text{C} \pm 1.87^\circ \text{C}$; min 16.07°C ; max 24.05°C), cold/low salinity
253 period ($15.73^\circ \text{C} \pm 1.87^\circ \text{C}$; min 11.30°C ; max 19.28°C) and cold/isolated lowest salinity events ($10.64^\circ \text{C} \pm 1.87^\circ \text{C}$; min
254 6.21°C ; max 14.19°C). Thus, from the two archaeological shells, the reconstructed

255 SST for Beg-an-Dorchenn may have roughly been around a mean 21 ± 2 ° C with extrema between 6 °
256 C (cold/punctual lowest salinity events) and 24° C (warm/high salinity event). All these values are
257 within the limitation range of 3 to 28° C to use the Böhm equation as well as in the SST range of 3.2° C
258 to 23.6° C (Mean 18.4° C) currently recorded at Loch River, 100 km East of Beg-an-Dorchenn, (Poulain
259 2010, Poulain et al. 2011).

260 III.4. Catch seasonality

261 BAD-5 shows its 4th and last annual notch very close to the ventral margin (11 days). On the other hand,
262 the BAD-18 shell shows 6 weeks of growth from the 4th annual break to the ventral margin. Thus BAD-
263 5 and BAD-18 shells were thus probably collected at the early spring period during the restart of growth
264 after winter growth break/reduction. We also estimated the season of collection with the quartile
265 method by comparing the $\delta^{18}\text{O}$ variation over the course of a year of growth and the $\delta^{18}\text{O}$ at the
266 outermost growing edge of the shells (Table 3). The upper quartile (>75%) of $\delta^{18}\text{O}$ values reflects the
267 lowest SST during winter (> -0.015 ‰; max 0.680 ‰; (N=30) and > 0.239 ‰; max 0.547 ‰; (N=18) for
268 BAD-5 and BAD-18 respectively). The last weeks of growth of BAD-5 and BAD-18 shells displayed $\delta^{18}\text{O}$
269 values close to the lower limit of the upper quartile (0.189 ‰ (N=1) and 0.303 ‰ (N=2) respectively).
270 Those stable isotope samples encompass a period of several weeks because of low growth rates. Thus,
271 although those isotope data show less temporal precision than the increment data, the sclerochemical
272 study also suggests a catch during early spring. This period of human occupation and mollusks feeding
273 are in accordance with seasonality from other zooarcheological remains of Beg-an-Dorchenn site such
274 as fishes and crabs (Dupont et al. 2010).

275 An intent to specify the growing months for *Ruditapes decussatus* archaeological shell was made using
276 both increment and isotope data. A year of growth was characterized as the number of growth
277 increments between two consecutive (winter) growth breaks. For each $\delta^{18}\text{O}$ shell value, the number
278 of days encompassing the isotope samples and the corresponding mean daily growth were calculated.
279 Then the calendar day of 15th of August (current highest SST) was attributed to the lowest $\delta^{18}\text{O}$ shell
280 value (highest SST). From this day, a calendar date for each couple increment/isotope sample was
281 generated (forwards and backwards). This work has been applied to the 3rd and 4th year of growth of
282 BAD-5 and to the 4th year of growth of BAD-18. During the 3rd year, BAD-5 grew between the beginning
283 of May and mid-November; the following year (4th) the growth starts at mid-march and stops at the
284 end of December. During its 4th year of growth BAD-18 grew from mid-April to early December. By
285 centering the growing days at mid-August, the shells of *Ruditapes decussatus* display a mean growing
286 season between early April and early December with a standard deviation is 3 to 4 weeks which is very
287 similar to the growing season of *Ruditapes philippinarum* from March to November (Poulain, 2010). It

288 has to be noted that the growth break between the 3rd and 4th year of growth of BAD-5 can be
289 estimated to 4 months which, with the duration of growth of the 3rd year of BAD-5 (7 months), allow
290 one to assess the complete growth activity pattern of BAD-5 during that year.

291 IV. Discussion

292 IV.1. Shell diagenesis and increment readability

293 The two shells of *Ruditapes decussatus* show a very high state of preservation at structural as well as
294 chemical and microstructure levels. This absence of apparent diagenesis allowed development of
295 sclerochronological and sclerochemical analyses on specimens dated between 5700 and 5500 Cal. BC.

296 IV.2. Growth parameters and life traits of Beg-an-Dorchenn *R. decussatus* specimens

297 Shell growth rhythm (number of daily increment) are usually species-specific and related to the
298 astronomical cycle (Sun-Moon-Earth tryptic) while shell growth amplitude (increment thickness
299 variation) is environmentally dependent (Gosselin et al. 2013). Detailed analysis of growth marks from
300 daily to annual periodicities allow one to determine a growth rhythm of two increments per day for
301 *Ruditapes decussatus*, similar to its close taxonomic relative *Ruditapes philippinarum* which follows a
302 tidal rhythm (Poulain et al. 2011). Following this hypothesis, the sections of *R. decussatus* shells in this
303 study grew 3.3 cm in 23 months (BAD-5) and 1 cm in 11 months (BAD-18). Thus, the great readability
304 of the growth increments gave access to up to 3 partial years of daily growth.

305 *Ruditapes decussatus* archaeological shells show a winter growth break from 2 to 7 months depending
306 on the year of growth. With annual recording/growing window periods between 5 and 10 months,
307 Beg-an-Dorchenn bivalves were probably growing from spring up to early winter when temperatures
308 were close to their physiological optimum and thus were recording maximal annual SST. However, they
309 did not record the minimum annual SST (winter growth break) leading to an overestimation of the
310 mean reconstructed temperature. Thus, the real SST occurring at Beg-an-Dorchenn and the potential
311 shift with current SST is difficult to currently assess.

312 We recommend to preferentially select *R. decussatus* specimens of 3-4 years old when the number of
313 growing days per year is the largest. Tidal growth bands analyses from annual growth breaks allow a
314 smaller uncertainty than isotope analyses (infra-daily VS 10 days) but sclerochemical analyses, by
315 revealing the lowest $\delta^{18}\text{O}$ shell value (highest SST), offer the possibility compare the growing period at
316 intra and inter specimen level as well as between different human occupation duration.

317

318 The duration of the annual break is inter and intra-species dependent (ontogeny) as well as
319 environmentally impacted (*e.g.* SST variations). However, this mean duration of growth breaks
320 between April and December (± 1 month) is similar to that of modern *Ruditapes philippinarum*
321 specimens of the same region (Loch River distant of ± 100 km from BAD site) which show a mean winter
322 growth break of 5 months between November and March (Poulain 2010). Sea and sediment
323 temperature along Atlantic French coasts usually range from minimum temperatures in February to
324 maximum temperature in August which respectively match the period of lowest and highest growth in
325 the Beg-an-Dorchenn shells confirming that the growth breaks occur in winter (Gómez-Gesteira et al.
326 2008).

327 However, restart of growth after the winter break is still not easy to determine in archaeological shells
328 as the duration of growth break is age-dependent and can also vary from year to year due to energy
329 reserves kept from the previous year (Chauvaud et al. 2012). That could be particularly the case during
330 the third year of growth of BAD-5 with a growing season of ten months suggesting that some extra
331 energy from the second year may have been used at the beginning of the third years and that a higher
332 part of the third year energy reserved may have been redirected for shell growth activity leading to a
333 longer growing season.

334 To gain insight of the particular annual growth of the archaeological specimens among the species
335 growth range, growth curves deducted from the four winter breaks of the studied shells were
336 calculated and then compared with length-at-age data of southern modern *Ruditapes decussatus*
337 populations (Figure 6.). Archaeological shells are smaller during their first and second years than the
338 populations growing in Atlantic southern France (Arcachon and Arguin Bays) or North-Eastern Adriatic
339 (Pag Bay) before reaching similar sizes during their 4th year of growth. The modern shells of *R.*
340 *decussatus* grew mainly during their first two years while the archaeological shells show a higher
341 growth rate later catching up with the modern ones during the 3rd and 4th years.

342 The growth discrepancy between modern and archaeological specimens could be explained by a
343 difference in life history-traits, timing events and energetic management (*e.g.* winter growth break,
344 size at first reproduction) driven directly or indirectly by climatic and environmental variations (*e.g.*
345 temperature variability, food availability VS population density, river fresh water VS oceanic marine
346 water or opened bay VS semi-closed embayment). Genetic variability could underlie such growth
347 variability patterns with appearance of different populations from successive glacial/interglacial
348 periods. Testing this hypothesis is beyond the scope of the present study.

349 The latitudinal factor acts as a driver of growth heterogeneity in bivalves (Sato 1999). Indeed Chauvaud
350 et al. (2012) show that Atlantic *Pecten maximus* population exhibit a lower growth rate and a higher

351 potential maximum size in higher latitude. This is also the case with the Northern Atlantic Mesolithic
352 shells of *R. decussatus* compared to the Southern Atlantic and Mediterranean modern populations.
353 Thermal gradient is closely related to the latitudinal gradient and acts on growth parameters such as
354 the mean daily growth increment thickness as well as the period of growing season. Disentangling the
355 latitudinal effect (space) from the temperature variations between the Mesolithic and current era stills
356 a challenge.

357 Finally, the growth patterns displayed by the Mesolithic specimens such as a low growth rate, a high
358 maximum size and growth break in winter tend to situated those individuals close to the Northern limit
359 of *R. decussatus* range.

360 V. Conclusion

361 Two specimens of the carpet shell *Ruditapes decussatus* from the Mesolithic shell midden of Beg-an-
362 Dorchenn were studied in order to assess their period of collection as well some insight into paleo-
363 temperature reconstruction.

364 This paper was firstly an attempt to adapt sclerochronological methods to archeological materials and
365 eventually use it routinely in further studies. Cross sectioned shells display very clear growth structures
366 allowing us to assess a growth rhythm of 2 increments per lunar day and to characterize daily growth
367 increments as well as winter annual growth breaks. The daily growth thickness and the annual growth
368 duration, are both ontogenetically and environmentally dependent. Sclerochronological and
369 sclerochemical results show that the *R. decussatus* studied shells were collected at early spring. Intra
370 and inter species analyses will help to strengthen the present results and to facilitate future
371 comparisons with other shell middens studied along European Atlantic coasts. We recommend to
372 preferentially select *R. decussatus* specimens of 3-4 years old when the number of growing days per
373 year is the largest. Moreover, additional chemical analysis (*e.g.* mapping) of growth dependent
374 elements such as Manganese, Magnesium, Strontium or Barium could help in the interpretation of
375 growth marks and temporal frameworks (Langlet et al. 2006, Poulain et al. 2015, Hausmann et al.
376 2019.).

377 A second approach of this paper was a climatic concern about the thermal variability of coastal oceanic
378 waters in the west part of France 7700 to 7500 years ago reconstructed from oxygen stable isotope
379 ratios. Sclerochemical analyses of shell carbonates were conducted to test the feasibility of such
380 analyses and display seasonal variability. Moreover, the range of reconstructed SST did not show
381 nonsensical values. However further interpretations are difficult to deduce from the present data.
382 Indeed, we must be careful to the uncertainties introduced into our results: the Böhm equation used

383 for SST reconstruction was of broad-spectrum including a large variety of marine invertebrates and the
384 $\delta^{18}\text{O}_w$ data could have been more geographically closer, restricting the understanding of the impact of
385 the salinity. Thus, specific SST- $\delta^{18}\text{O}_{\text{shell}}$ and Salinity- $\delta^{18}\text{O}_w$ equations could be developed for *Ruditapes*
386 *decussatus* from the Beg-an-Dorchenn shell midden and its surrounding waters in order to reduce
387 some uncertainties in future $\delta^{18}\text{O}$ analyses.

388 Recorders of different environmental and ecological parameters will lead to a better understanding of
389 past climate variations and could specify how far the Mesolithic sea temperatures were different from
390 the current ones. *R. decussatus* is particularly suited to address paleo-environmental issues at high
391 resolutions such as the seasonal periodicity.

392 To conclude, this paper is a first study on the carpet shell *Ruditapes decussatus* from an archaeological
393 context. These promising results are an incentive to extend these investigations in the others Beg-an-
394 Dorchenn archaeological levels and on the whole excavated area. Such a high spatio-temporal level of
395 analyses is fundamental to better understand the rhythm of residence of these late hunter-gatherer-
396 fishers on the French Atlantic coast. Additional sclerochronological and chemical research on
397 Mesolithic and modern mollusk species along the European Atlantic coast will also contribute to the
398 problematic seasonal occupation as well as climate variability at the Mesolithic-Neolithic transition.

399 **VI. Acknowledgments**

400 The authors thank two anonymous reviewers for their thorough and insightful comments and
401 suggestions. The authors thank J. Le Lannic from university of Rennes 1 and J.-F. Bardeau from
402 university of Le Mans for technical assistance respectively in SEM and in Raman analysis. Thanks to J.
403 Thiebault (UBO-LEMAR) for the Isotopic analysis process and Prof. B. Schöne (Univ. Gutenberg-Mainz)
404 for the spectrometer facilities. The authors sincerely acknowledge K. Buquen and W. Grey for the
405 language editing. This work was supported by the EPT of the European University of Brittany
406 PROXARCHEOBIO - France (2010-2012 / CReAAH-LEMAR Leader C Dupont), the scientific challenges of
407 the University of Rennes 1 « SMS Shell-Middens Seasonality (2017 / Leader C. Dupont) », private
408 donations (2017) and by the CReAAH laboratory.

409 **VII. Author contributions**

410 Conceptualization CD, MG, YMP; Methodology CD, CeP, FP, GM, MG, XLC, YG; Formal analysis MG;
411 Investigation CD, CeP, ChP, FP, GM, MG, XLC, YG; Resources CD, CeP, FP, GM, MG, XLC, YG; Writing -
412 Original Draft CD, MG; Writing - Review & Editing CD, ChP, GM, MG, YMP; Visualization CD, MG;
413 Supervision CD; Project administration CD; Funding acquisition CD, MG.

414 **VIII. Declaration of interest**

415 Declarations of interest: none.

416 **VIII. References**

- 417 Andrus C.F. 2011. Shell midden sclerochronology. *Quaternary Science Reviews*. 30 : 2892–2906.
- 418 Bar-Yosef Mayer D. E. (ed.). 2005. 9th ICAZ Conference, Durham 2002, *Archaeomalacology: Molluscs*
419 *in former environments of human behaviour*, Oxford: Oxbow Books 184p.
- 420 Bessat F., Tabeaud M. 1998. La croissance corallienne : un marqueur des environnements actuels et
421 passés. *Annales de Géographie*. 599 : 16–32.
- 422 Böhm F., Joachimski M., Dullo W., Eisenhauer A., Lehnert H., Reitner J., Worheide G. 2000. Oxygen
423 isotope fractionation in marine aragonite of coralline sponges. *Geochimica et Cosmochimica Acta* 64
424 (10) : 1695-1703.
- 425 Brock V., Bouget E. 1989. Analyses of shell increment and microgrowth band formation to establish
426 seasonality of Mesolithic shellfish collection. *Journal of Danish Archaeology*. 8: 7-12.
- 427 Buddemeier, R. 1978. Sclerochronology: a data source for reef systems models. *Atoll Research Bulletin*.
428 220 (4) : 25–32.
- 429 Chauvaud, L., Lorrain, A., Dunbar, R.B., Paulet, Y.-M., Thouzeau, G., Jean, F., Guarini, J.-M., Mucciarone,
430 D., 2005. Shell of the Great Scallop *Pecten maximus* as a high-frequency archive of paleoenvironmental
431 changes. *Geochemistry, Geophysics, Geosystems*. 6 (Q08001).
- 432 Chauvaud, L., Patry, Y., Jolivet, A., Cam, E., Le Goff, C., Strand, Ø., Charrier, G., Thébault, J., Lazure, P.,
433 Gotthard, K., Clavier, J., 2012. Variation in size and growth of the great scallop *Pecten maximus* along
434 a latitudinal gradient. *PLoSOne* 7 (5), e37717.
- 435 Claassen C. 1998. *Shells*. Cambridge manuals in archaeology. Cambridge University Press, Cambridge
436 263p.
- 437 Dang C. 2009. Dynamique des populations de palourdes japonaises (*Ruditapes philippinarum*) dans le
438 bassin d'Arcachon : conséquences sur la gestion des populations exploitées. Thèse de doctorat de
439 l'université de Bordeaux 1. 374p.
- 440 Deith R. 1983. Molluscan Calendars: The use of Growth-line Analysis to Establish Seasonality of
441 Shellfish Collection at the Mesolithic Site of Morton, Fife. *Journal of Archaeological Science*. 10 (5) :
442 423-440.

443 Du Chatellier P. 1881. Exploration des tumulus de Run-Aour et de la Torche en Plomeur (Finistère) et
444 du Kjökkenmödding de la Torche. Mémoires de la Société d'émulation de Côtes-du-Nord. XIX : 175-
445 182.

446 Dupont C. 2006. La malacofaune de sites mésolithiques et néolithiques de la façade atlantique de la
447 France : Contribution à l'économie et à l'identité culturelle des groupes concernés. British
448 Archaeological Reports. International Series. 1571. 438p.

449 Dupont C. 2016. Could occupation duration be related to the diversity of faunal remains in Mesolithic
450 shell middens along the European Atlantic seaboard? Quaternary International. 407 : 145-153.

451 Dupont C., G. Marchand, (dir.). 2016. Archéologie des chasseurs-cueilleurs maritimes. De la fonction
452 des habitats à l'organisation de l'espace littoral / Archaeology of maritime hunter-gatherers. From
453 settlement function to the organization of the coastal zone. Séances de la Société préhistorique
454 française. 6. 425 p.

455 Dupont C., Marchand G., Carrion Y., Desse-Berset N., Gaudin L., Gruet Y., Marguerie D., Oberlin C. 2010.
456 Beg-an-Dorchenn : une fenêtre ouverte sur l'exploitation du littoral par les peuples mésolithiques du
457 sixième millénaire dans l'ouest de la France. Bulletin de la Société Préhistorique Française. 107 (2) :
458 227-290.

459 Dupont C., Tresset A., Desse-Berset N., Gruet Y., Marchand G., Schulting R. 2009. Harvesting the
460 seashores in the Late Mesolithic of north-western Europe. A view from Brittany? Journal of World
461 Prehistory. 22 (2) : 93-111.

462 Epstein S., Mayeda T. 1953. Variation of O^{18} content of waters from natural sources.
463 *Geochimica et Cosmochimica Acta*. 4 (5) : 213-224.

464 Gómez-Gesteira, M., decastro, M., Alvarez, I., Gomez-Gesteira, J.L., 2008. Coastal sea surface
465 temperature warming trend along the continental part of the Atlantic Arc (1985–2005). *J. Geophys.*
466 *Res : Oceans*. 113 (C4).

467 Gosling E. 2003. Bivalve molluscs: biology, ecology and culture. Oxford, OX2, OEL, UK. 443p.

468 Gosselin M., Lazareth C.E., Dufour E., Guzman N., Ortlieb. L. 2007. Improvement of image analysis for
469 sclerochronological and paleo-environmental studies on mollusc shells and fish otoliths. Presented at
470 the First International Conference on Sclerochronology. St Petersburg, FL.

471 Gosselin M., Lazareth C.E., Ortlieb L. 2013. Schlerochronological studies in the Humboldt Current System,
472 a highly variable ecosystem. *Journal of shellfish research*. 32 (3): 857-882.

473 Gutiérrez-Zugasti I., Andersen S.H., Araujo A. C., Dupont C., Milner N., Monge-Soares A.M. 2011. Shell
474 midden research in Atlantic Europe: state of art, research problems and perspectives for the future.
475 Quaternary International. 239 : 70-85.

476 Hausmann N., Robson H.K., Hunt, C. 2019. Annual Growth Patterns and Interspecimen Variability in
477 Mg/Ca Records of Archaeological *Ostrea edulis* (European Oyster) from the Late Mesolithic Site of
478 Conors Island. Open Quaternary, 5(1) : 9.

479 Jones D. S. 1983. Sclerochronology: reading the record of the molluscan shell. American Scientist. 71
480 (4) : 384–391.

481 Jurić I., Bušelić I., Ezgeta-Balić D., Vrgoč N., Peharda M. 2012. Age, growth and condition index of
482 *Venerupis decussata* (Linnaeus, 1758) in the Eastern Adriatic Sea. Turkish Journal of Fisheries and
483 Aquatic Sciences 12 (3) : 431-436.

484 Langlet D., Alunno-Bruscia M., De Rafélis M., Renard M., Roux M., Schein, E., Buestel D. 2006.
485 Experimental and natural manganese-induced cathodoluminescence in the shell of the Japanese
486 oyster *Crassostrea gigas* (Thunberg, 1793) from Thau Lagoon (Hérault, France): ecological and
487 environmental implications. Marine Ecology Progress Series. 317 : 143-156.

488 Le Treut Y. 1986. La palourde. Anatomie - Biologie - Elevage - Pêche - Consommation -Inspection
489 sanitaire. Thèse de Doctorat. Nantes. Ecole Nationale Vétérinaire. 161p.

490 Mannino M.A., Spiro B.F., Thomas K.D. 2003. Sampling shells for seasonality: oxygen isotope analysis
491 on shell carbonates of the inter-tidal gastropod *Monodonta lineata* (da Costa) from populations across
492 its modern range from a Mesolithic site in southern Britain. Journal of Archaeological Science. 30 (6) :
493 667-679.

494 Marchand G., Dupont C., Oberlin C., Delque-Kolic E. 2009. Chapter Sixteen : Entre « effet réservoir » et
495 « effet de plateau » : la difficile datation du Mésolithique de Bretagne. In: Ph. Crombé, M. Van
496 Strydonck, J. Sergant, M. Bats & M. Boudin (eds.), Proceedings of the international congress
497 “Chronology and Evolution in the Mesolithic of NW Europe”, Brussels, May 30 - June 1 2007. Cambridge
498 Scholar Publishing. 307-335.

499 Milner N., 2005. Seasonal Consumption Practices in the Mesolithic: Economic, Environmental, Social
500 or Ritual? In: Milner N., Woodman P. (eds.). Mesolithic Studies at the beginning of the 21st Century.
501 Oxbow Books. 56-68.

502 Milner N., Craig O.E., Bailey G.N. (eds.). 2007. Shell-Middens in Atlantic Europe. Oxbow books. 336p.

503 Moss M. L. 1993. Shellfish, gender, and status on the Northwest coast: reconciling archeological,
504 ethnological, and ethnohistorical records of the Tlingit. *American Anthropologist*. 95 (3) : 631-652.

505 Poulain C. 2010. Potentiel de la palourde japonaise comme traceur environnemental : vers une
506 compréhension des mécanismes de transfert des signaux environnementaux au sein des structures
507 carbonatées biogènes. Thèse de l'Université de Brest. 182p.

508 Poulain C., Lorrain A., Mas R., Gillikin D.P., Dehairs F., Robert R., Paulet Y.-M. 2010. Experimental shift
509 of diet and DIC stable carbon isotopes: Influence on shell $\delta^{13}\text{C}$ values in the Manila clam *Ruditapes*
510 *philippinarum*. *Chemical Geology* 272 (1-4) : 75–82.

511 Poulain C., Lorrain A., Flye-Sainte-Marie J., Amice E., Morize E., Paulet Y.-M. 2011. An environmentally
512 induced tidal periodicity of microgrowth increment formation in subtidal populations of the clam
513 *Ruditapes philippinarum*. *Journal of Experimental Marine Biology and Ecology*. 397 (1) : 58–64.

514 Poulain C., Gillikin D.P., Thebault J., Munaron J.-M., Bohn M., Robert R., Paulet Y.-M., Lorrain A. 2015.
515 An evaluation of Mg/Ca, Sr/Ca, and Ba/Ca ratios as environmental proxies in aragonite bivalve shells.
516 *Chemical Geology*. 396 : 42-50.

517 Prendergast A.L., Stevens R.E., O'Connell T.C., Fadlalak A., Touati M., Al-Mzeine A., Schone, B.R., Hunt
518 C.O. and Barker, G. 2016. Changing patterns of eastern Mediterranean shellfish exploitation in the Late
519 Glacial and Early Holocene: Oxygen isotope evidence from gastropod in Epipaleolithic to Neolithic
520 human occupation layers at the Haua Fteah cave, Libya. *Quaternary International*. 407 (B) : 80-93.

521 Quérou J.-C., Vayne J.-J. 1998. Les fruits de la mer et plantes marines des pêches françaises. Les
522 encyclopédies du naturaliste. Delachaux et Niestlé. 256p.

523 Sato S. 1999. Temporal change of life-history traits in fossil bivalves: an example of *Phacosoma*
524 *japonicum* from the Pleistocene of Japan. *Paleogeography, Paleoclimatology, Paleoecology*. 154 (4) :
525 313–323.

526 Schaffer P., Fortunato H., Bader B., Liebetrau V., Bauch T., Reijmer J. J. G. 2011. Growth rates and
527 carbonate production by coralline red algae in upwelling and non-upwelling settings along the Pacific
528 coast of Panama. *Palaios*. 26 (7) : 420–432.

529 Schöne B. R. 2008. The curse of physiology: challenges and opportunities in the interpretation of
530 geochemical data from mollusk shells. *Geo-Marine Letters*. 28 : 269–285.

531 Sobral P., Widdows J. 1997. Effects of elevated temperatures on the scope for growth and resistance
532 to air exposure of the clam *Ruditapes decussatus* (L.), from southern Portugal. *Scientia Marina* 61 (1) :
533 163-171.

534 Szabó K., Dupont C., Dimitrijevic V., Gastélum Gómez L. G., Serrand N., (eds.) 2014.
535 Archaeomalacology: Shells in the Archaeological Record. Proceedings of the 11th ICAZ International
536 Conference. Paris - Archaeomalacology Working group, 23-28 August 2010, France. British
537 Archaeological Reports. 2666.

538 Testart A., 1982. Les chasseurs-cueilleurs ou l'origine des inégalités. Éditions de la Société
539 d'Ethnographie. 254 p.

540 Thomson D. F., 1939. The seasonal factor in human culture illustrated from the life of a contemporary
541 nomadic group. Proceedings of the Prehistoric Society. 5 (2) : 209 -221.

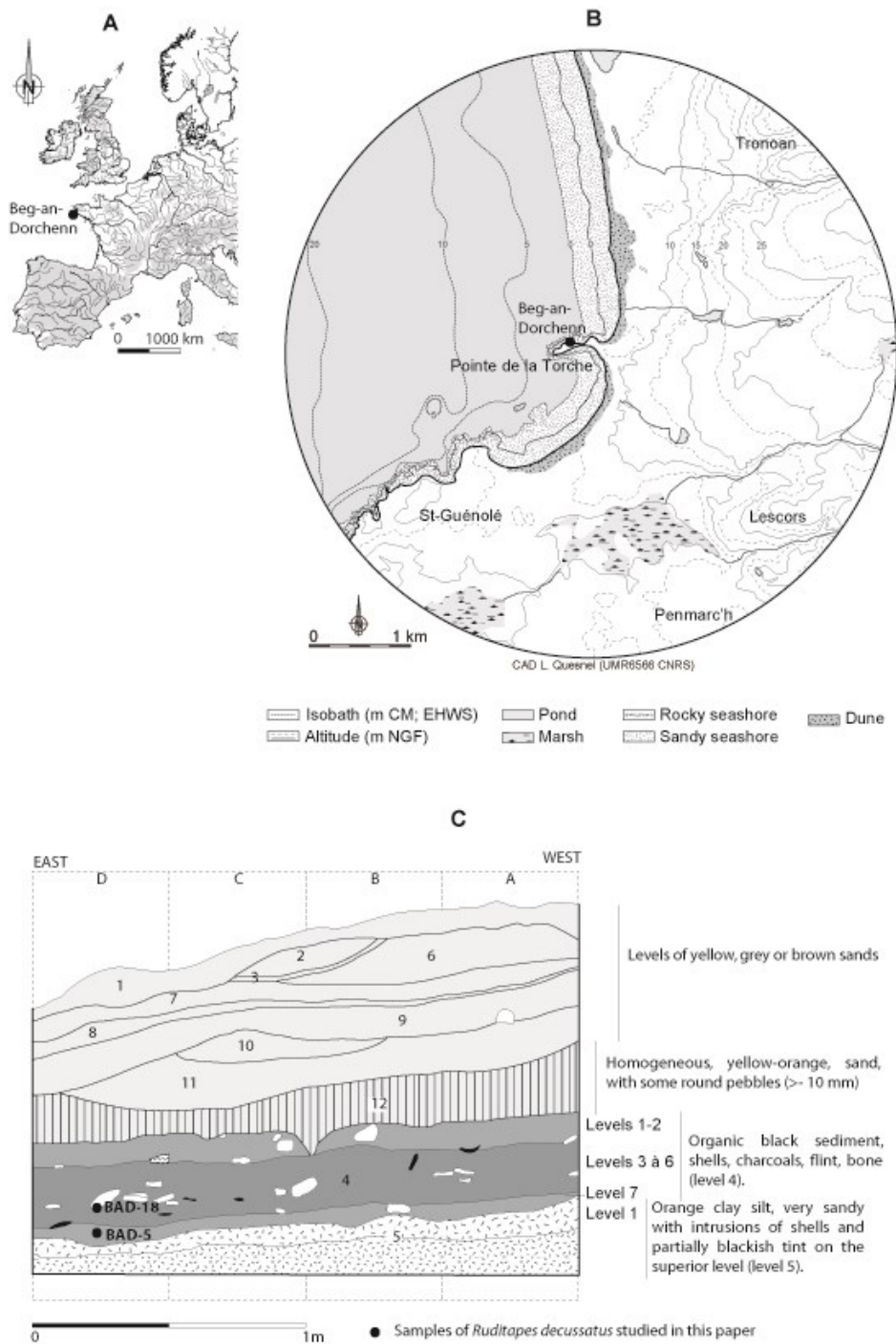
542 Trinkler N., Bardeau J.F., Marin F., Labonne M., Jolivet A., Crassous P., Paillard C. 2011. Mineral phase
543 in the shell repair in the Manila clam *Ruditapes philippinarum* affected by the Brown Ring Disease: a
544 Raman micro-spectrometry, Scanning Electron Microscopy and hemocyte cellular study. Diseases of
545 aquatic organisms. 93 (2) : 149–162.

546 Urey, H., Lowenstam, H., Epstein, S., McKinney, c. 1951. Measurement of paleotemperatures and
547 temperatures of the upper Cretaceous of England, Denmark, and the southeastern United States.
548 Geological Society of America Bulletin. 62 (4) : 399-416.

549 Wanamaker, A. D., K. J. Kreutz, B. R. Schöne & D. S. Introne. 2011. Gulf of Maine shells reveal changes
550 in seawater temperature seasonality during the Medieval Climate Anomaly and the Little Ice Age.
551 Paleogeography, Paleoclimatology, Paleoecology. 302 (1-2) : 43–51.

552 Yesner D.R. 1980. Maritime hunter gatherers: ecology and prehistory. Current Anthropology. 21 (6) :
553 727-750.

554 Zvelebil M. (dir.) 1986. Hunters in transition. Mesolithic societies of temperate Eurasia and their
555 transition to farming. Cambridge University Press. p194.



556

557 Figure 1: A. Location map of the shell midden of Beg-an-Dorchenn B. in the present marine
 558 environment (CAD L. Quesnel); C. Stratigraphy of the 2001 survey (CAD G. Marchand).

559

A



B



C



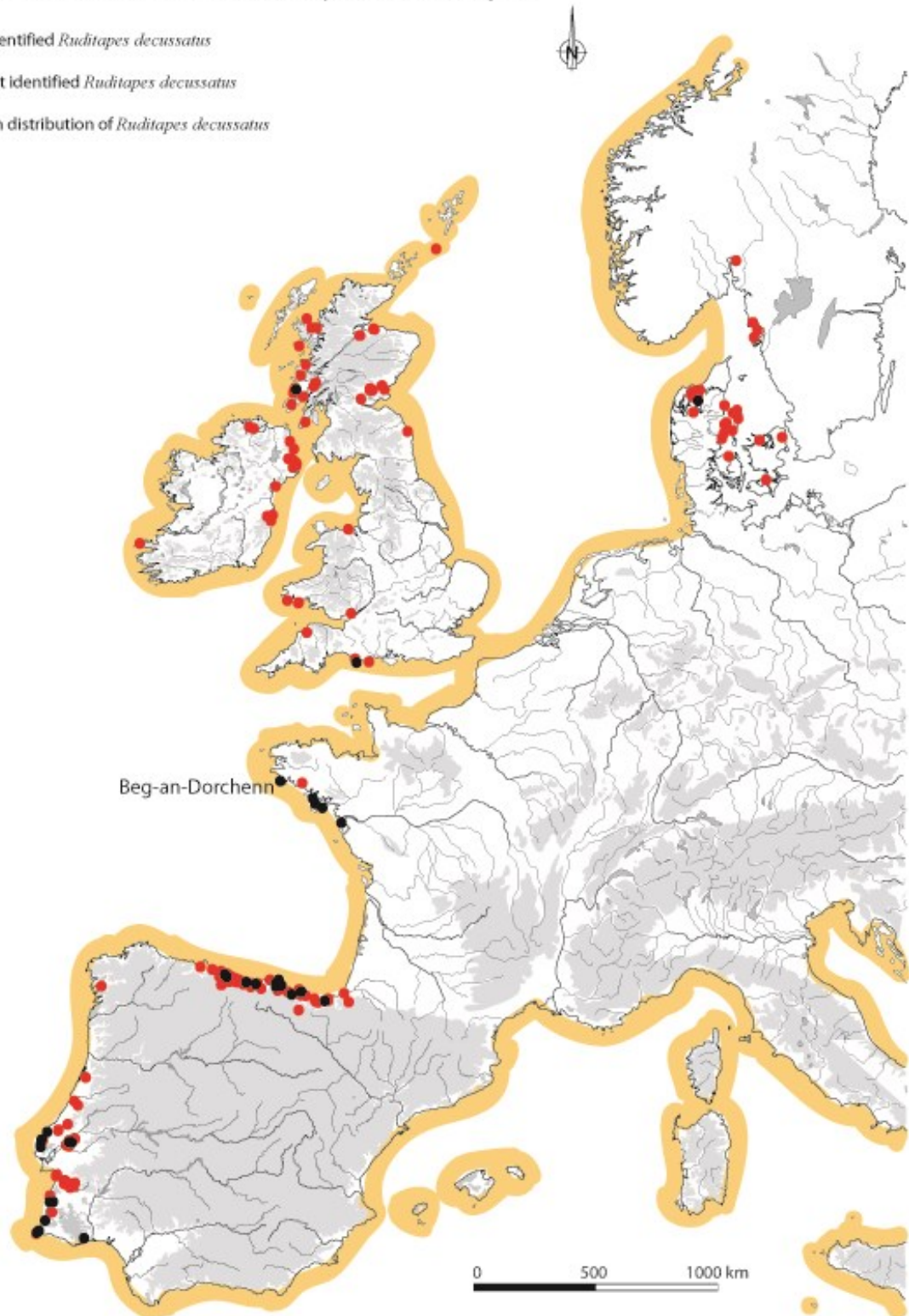
560

561 Figure 2: Detail of the shell midden of Beg-an-Dorchenn; A. survey in 2001; B. detail of the shell midden
562 in May 2001; C. Coarse mesh of sieving process (Credit C. Dupont).

563

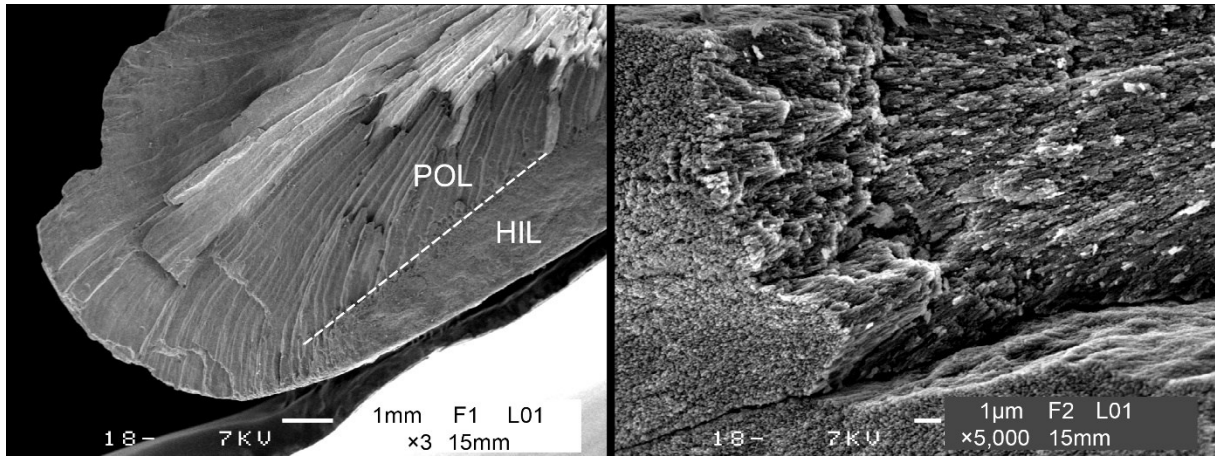
Mesolithic shell-middens of the European Atlantic façade

- With identified *Ruditapes decussatus*
- Without identified *Ruditapes decussatus*
- Modern distribution of *Ruditapes decussatus*



564

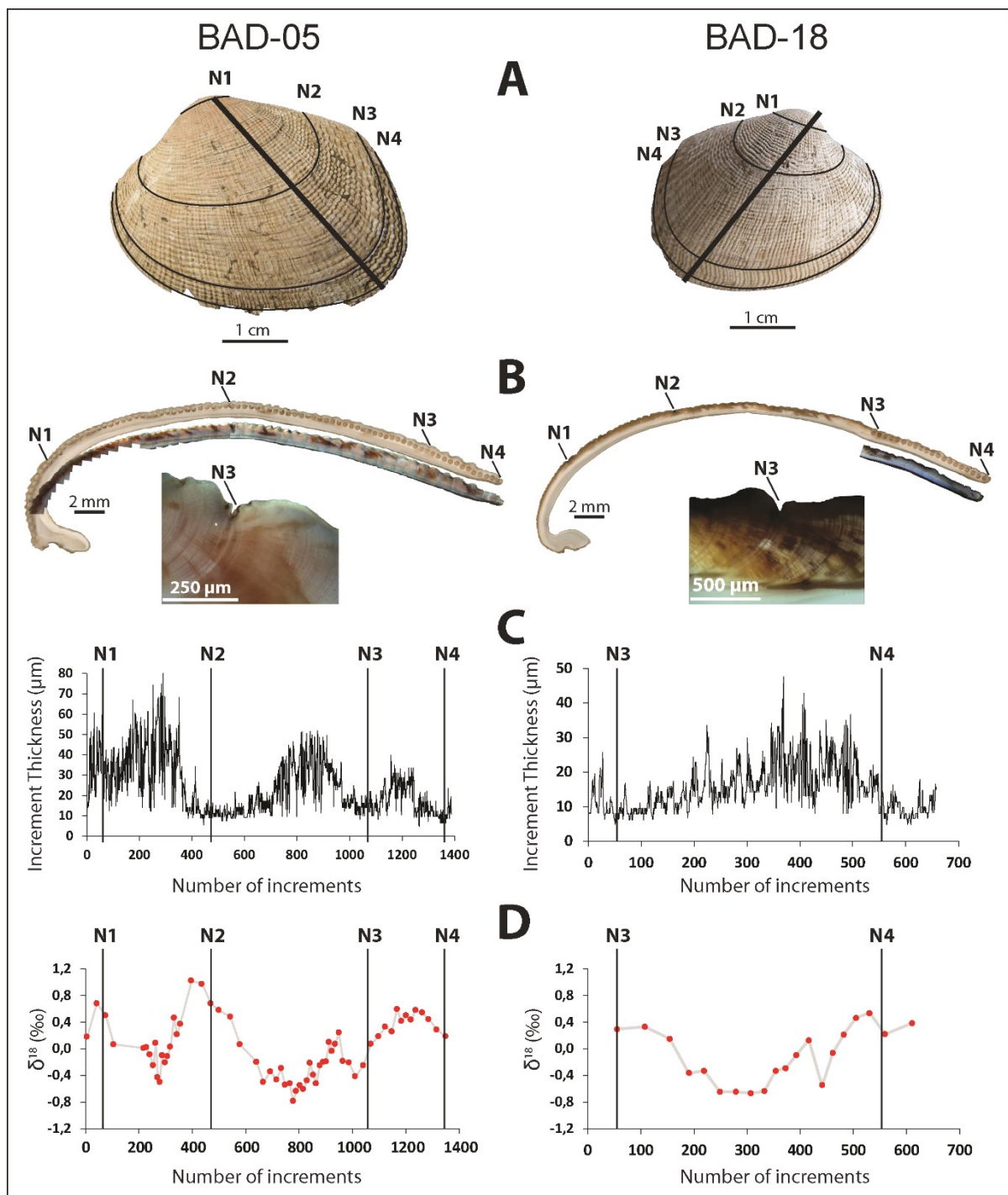
565 Figure 3: Map of the Mesolithic shell-middens along the European Atlantic coast with the modern and
566 archaeological presence of *Ruditapes decussatus* (Data 2017, unpublished C. Dupont).



567

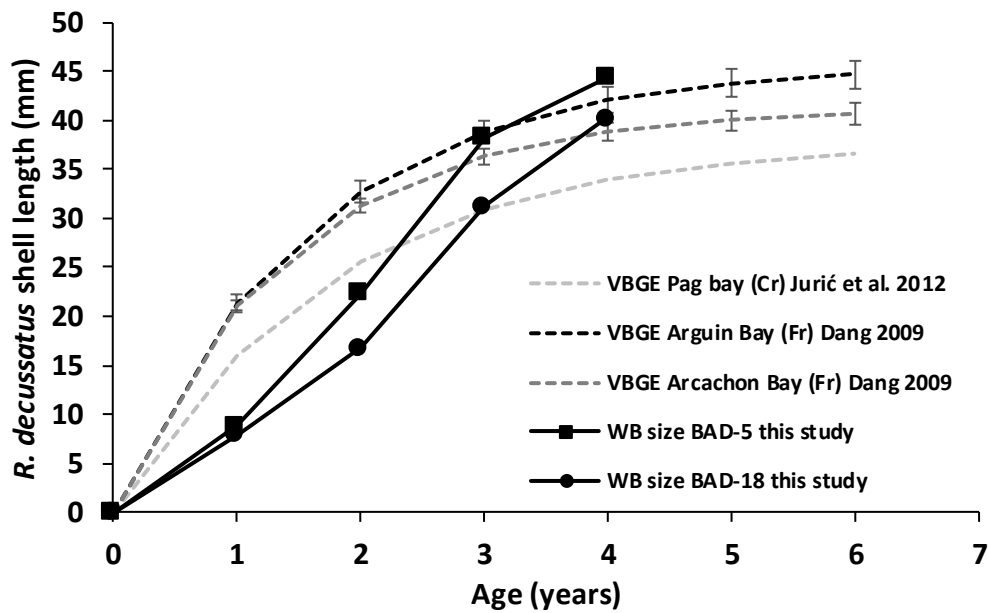
568 Figure 4: SEM images of shell samples (BAD-18) manually broken in order to observe aragonitic
569 structures along the longitudinal and transversal growth axis. Left image: Calcium carbonate crystals
570 show a homogeneous inner layer (HIL) and a prismatic outer layer (POL). Right image: detail of the
571 prismatic layer. Except slightly less sharpened crystal side and apex than modern shells, no sign of
572 diagenesis has been detected. White scale bar: 1 mm (left image) and 1µm (right image) (Credit: J. Le
573 Lannic).

574



576

577 Figure 5: Sclerochronological and geochemical analysis of the *Ruditapes decussatus* shells BAD-5 (left)
 578 and BAD-18 (right). A. The well-preserved archaeological valves with annual marks (*i.e.* winter breaks)
 579 and fortnightly concentric ridges at the shell surface. B. Cross sections with isotopic samples (upper)
 580 and growth lines (lower). A snapshot of one characteristic winter break is provided for each valve
 581 (white bar scale of 250 µm). C. Growth increment thickness variation. D. $\delta^{18}\text{O}_{\text{shell}}$ isotopic values (Red
 582 spots). Annual notches (N1-N4 and vertical solid lines).



584

585 Figure 6: Length-at-age data of the bivalve *Ruditapes decussatus*. Comparison between winter break
 586 (WB) sizes of Beg-an-Dorchenn archaeological specimens BAD-5 and BAD-18 (Table 1. N1-N4) and Von
 587 Bertalanffy growth equation (VBGE) of modern European population. East Atlantic South France
 588 population (Arguin and Arcachon) from Dang 2009 and North East Adriatic population from Jurić et al.
 589 2012. The Height-at-age to Length-at-age transformation of archaeological shell data was estimated
 590 from the relationship described in Jurić et al (2012). Standard deviation in vertical bars.

591

592 Table 1: Growth parameters (μm) for the two studied valves of *Ruditapes decussatus*. Increment
 593 parameters; SD standard deviation. External annual growth marks parameters along the maximum
 594 growth axe; N1-N4: Number 1 to 4 notches (Cf. Figure 5-A); VM: ventral margin.

	N increment	Mean	SD	Min	Max	N1	N2	N3	N4	VM
BAD-5	1388	23.96	13.4	4.68	83.09	6.61	15.63	26.25	30.26	30.56
BAD-18	657	15.07	7.03	4.8	47.5	5.98	11.9	21.55	27.51	27.72

595

596

597

598 Table 2: $\delta^{18}\text{O}_{\text{Shell}}$ parameters (‰) for the two studied valves of *Ruditapes decussatus*. SD: standard
599 deviation.

	N $\delta^{18}\text{O}_{\text{Shell}}$	Mean	SD	Min	Max	Median
BAD-5	63	0.02	0.42	-0.78	1.02	0.02
BAD-18	20	-0.09	0.41	-0.66	0.55	-0.08

600

601

602

603 Table 3: Quartile method to assess the season of shellfish collection through the study of the annual
 604 range of the $\delta^{18}\text{O}_{\text{Shell}}$ (‰). BAD-5 data (N=30) come from the 3rd year of growth over 10 months. BAD-
 605 18 data (N=18) come from the 4th year of growth over 9 months.

	Quartile ranges	BAD-5 $\delta^{18}\text{O}$ (‰)	BAD-18 $\delta^{18}\text{O}$ (‰)	Inferred season
Quartile Model	Maximun value	0.68	0.547	winter
	75th percentile	-0.015	0.238	winter
	Median	-0.25	-0.19	Autumn/Spring
	25th percentile	-0.505	-0.573	Summer
	Minimun value	-0.78	-0.663	Summer
Time of collection	Last weeks of growth	0.189	0.303	Late Winter / Early Spring

606

607

1 Supplementary material 1 : Detailed methodology

2 SP1.1. Beg-an-Dorchenn excavation protocol in 2001.

3 The excavation realised in 2001 at Beg-an-Dorchenn consisted in sampling the whole sediment of 1m³
4 of the shell-midden by horizontal levels (thickness: 5 cm) and per quarter of square meter (Dupont et
5 al. 2010). In a second step, the sediment was sieved (5 and 1.6 mm) with fresh water in a laboratory.
6 The whole fraction of the taller mesh and only a small fraction of the fine mesh (50 ml of a quarter of
7 square meter) have been sorted. A first evaluation of the season of gathering of the carpet shell has
8 been made at Beg-an-Dorchenn after an external observation of the growth rate of 299 fragments
9 from the squares A and C of the 2001 excavation (Dupont 2006). This observation led to the conclusion
10 of a capture window between the winter and end of spring. (Dupont 2006). Unfortunately, this method
11 remains rough and new developments in biology can be adapted to archaeological samples to have a
12 better precision of the date of collection of the shell linked to climatic data. this observation lead to
13 the sclerochronological and sclerochemical approach developed in this paper.

14 SP1.2. Shell structural analysis SEM and Raman

15 Prior to any growth structure studies (*e.g.* growth increment), microstructural and chemical analyses
16 need to be carried out on the calcium carbonated shells in order to deal with diagenesis potential
17 issues (Nouet et al. 2015). Indeed, structural and chemical changes in the bivalve shell specimen may
18 appear after its death and lead to a lower increment readability and/or to a misinterpretation of
19 subsequent geochemical analysis (Nouet et al. 2015). Mainly, diagenesis affects the crystal structure
20 of the calcium carbonate and modifies its form from aragonite into calcite.

21 Shell structural concerns have been observed by Scanning electron microscope and chemical analysis
22 by Raman spectrometry. (JSM-6310F Scanning microscope JEOL) from a shell sample metallized with a
23 20/80 Palladium/Gold coat. Chemical analysis of the calcium carbonate form was provided by Raman
24 spectroscopy (T64000 Jobin-Yvon-Horiba) following the same analysis performed in manila clams,
25 *Ruditapes philippinarum* (Trinkler et al. 2011). It is a non-destructive technic of investigation using an
26 Argon-Krypton laser at a micrometer level and based on the shift of its energy when interacting with
27 molecular vibrations of the studied material (hereby the mollusk shell).

28 Additional references from supplementary material

29 Nouet J., Chevillard C., Farre B., Nehrke G., Campmas E., Stoetzel E., El Hajraoui M.A. , Nespoulet R.,
30 2015. Limpet Shells from the Aterian Level 8 of El Harhoura 2 Cave (Temara, Morocco): Preservation
31 State of Crossed-Foliated Layers. PLoS ONE, Public Library of Science. pp.0137162.